Inorganica Chimica Acta 376 (2011) 95–104

Contents lists available at ScienceDirect

Inorganica Chimica Acta

journal homepage: www.elsevier.com/locate/ica

Studies on the structure and properties of nickel complexes in a set of amide-based 13-membered macrocyclic ligands

Savita K. Sharma, Rajeev Gupta *

Department of Chemistry, University of Delhi, Delhi 110 007, India

ARTICLE INFO

Article history:
Received 31 January 2011
Received in revised form 21 May 2011
Accepted 2 June 2011
Available online 13 June 2011

Keywords:
Nickel
Macrocyclic ligands
Crystal structures
Electrochemistry

ABSTRACT

This work reports a systematic investigation to understand the structural, spectroscopic and redox properties of Ni(II) ion in a set of 13-membered amide-based macrocyclic ligands. Four macrocyclic ligands containing e^--donating/withdrawing substituents and their Ni(II) complexes have been synthesized and characterized. Structural analysis shows that the macrocyclic ligands create a square-planar environment and nicely accommodate the Ni(II) ion. Electrochemical results suggest that the complexes are capable of undergoing metal-centered oxidation. The electron-donating substituents on ligand lowers the redox potentials and better stabilizes the +3 oxidation state of metal. The electrochemically generated Ni^{III} species are shown to have rich spectroscopic features. For majority of complexes, the oxidized species are concluded to be Ni^{III} by their anisotropic EPR spectra typical for Ni^{III} ion in square-planar geometry. The absorption and EPR spectra for nickel complex bearing an –OMe group on the ligand; however, suggest a Ni(II) complex with a ligand-based radical.

1. Introduction

There has been considerable research interest to understand the role of redox-active transition metal ions in metalloenzymes [1–7]. In particular, the interest in the coordination and redox chemistry of nickel ion in variable oxidation states is important with implications in chemistry and biology [1–7]. This attention has been further renewed due to the participation of Ni^{3+} species in the redox catalytic cycle of several metalloenzymes [8–12]. Thus, a good number of well-characterized high-valent nickel complexes with diverse ligand types and coordination geometries are available [13–32]. Prominent among them are the square-planar Ni^{3+} complexes of amidate-containing ligands from the groups of Margerum et al. [21–24], Collins et al. [13,14,25,26], Kruger and Holm [15–19]; and Ruiz-Garcia and Journaux [27–31]; and octahedral Ni^{2+}, Ni^{3+}, and Ni^{4+} complexes with a common pyridine–amide ligand from Patra and Mukherjee [32]. In addition to the redox participation of a metal ion, certain redox-active ligands add a new dimension to the electron transfer processes [32–48]. In this category, redox non-innocence of *o*-phenylenediamine fragment when coordinated to a metal ion has been a major focus of study [33,36–48]. The extended conjugation of *o*-phenylenediamine fragment in a complex may alter the redox properties as it involves both metal and ligand based orbitals. In this regard, an investigation to assess the possible role of *o*-phenylenediamine-based ligands in the stabilization of high-valent metal complexes has been initiated by us recently [49–55]. Our goal is to understand the factors that contribute towards the stability of metal ions in high oxidation states, whereby not only the metal but also the associated ligand can serve as the electron reservoir. The present study is in continuation of our earlier work on the coordination chemistry and redox investigation of transition metals with amide-based macrocyclic ligands (complexes **A**–**J**, Scheme 1) [49,50] and their open-chain analogs (complexes **K**–**M**, Scheme 1) [51–55]. These macrocyclic ligands and their open-chain analogs have been shown to stabilize +2 as well as +3 oxidation states of the nickel ion in a square-planar geometry [49–51]. Further, the macrocyclic ligands have also been used to stabilize $Cu^{2+/3+}$ states in a square-planar environment [50]. Herein, we extend our earlier work [49,50] on 12-membered macrocyclic chemistry (complexes **A**–**J**, Scheme 1) and have expanded the ring size of the macrocycle to 13-membered. The expansion of macrocyclic ring size from 12-membered to 13-membered may help to understand the placement of metal ion within the macrocyclic cavity and its consequences on the structural and redox properties of the nickel ion. In addition, few macrocyclic ligands have also been synthesized carrying e^--donating/withdrawing substituents ($-CH_3$, –Cl, and $-OCH_3$) to investigate their effect on the relative stability of $Ni^{2+/3+}$ states. Finally, in continuation with our earlier work [49,50], the emphasis has been given to understand the effect of ligand architecture on the structure, properties and redox chemistry of nickel ion.

---

* Corresponding author. Fax: +91 11 2766 6605.
E-mail address: rgupta@chemistry.du.ac.in (R. Gupta).

0020-1693/$ - see front matter © 2011 Elsevier B.V. All rights reserved.
doi:10.1016/j.ica.2011.06.011

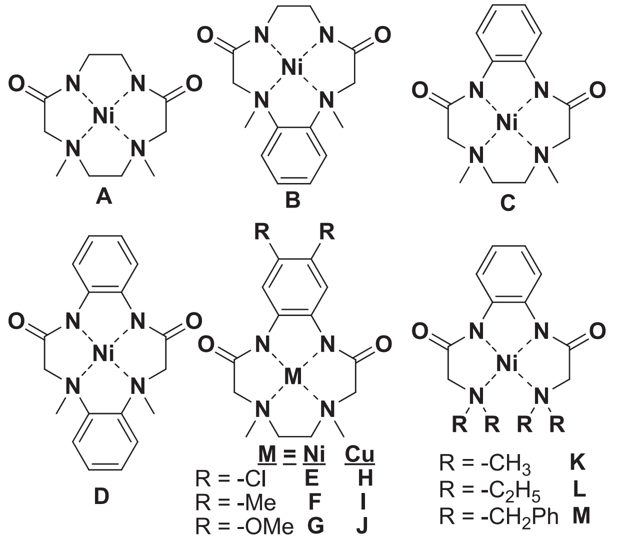

Scheme 1. Ni(II) and Cu(II) complexes with our earlier amide-based ligands.

2. Experimental

2.1. Materials and reagents

All reagents were obtained from the commercial sources and used as received. Solvents were purified as reported earlier [49–54]. The *N*,*N*′-bis(chloroacetyl)-*o*-phenylenediamine, *N*,*N*′-bis(chloroacetyl)-4,5-dichloro-*o*-phenylenediamine, *N*,*N*′-bis(chloroacetyl)-4,5-dimethyl-*o*-phenylenediamine, and *N*,*N*′-bis(chloroacetyl)-4,5-dimethoxy-*o*-phenylenediamine were prepared as reported in the literature [15,49,50,56].

2.2. Physical measurements

The conductivity measurements were done in organic solvents using the digital conductivity bridge from Popular Traders, India (model number: PT-825). The microanalytical data were obtained from the Elementar Analysen Systeme GmbH Vario EL-III instrument. The NMR measurements were done using either Hitachi R-600 FT NMR (60 MHz) or an Avance Bruker (300 MHz) instrument. The infra-red spectra (either as KBr pellet or as a mull in mineral oil) were recorded using the Perkin–Elmer FTIR-2000 spectrometer. The absorption spectra were recorded with the Perkin–Elmer *Lambda*-25 spectrophotometer. X-band EPR spectra were recorded on a Varian 109C or a Bruker EMX 1444 spectrometers (fitted with quartz Dewar for measurements at 120 K). The EPR spectra were calibrated with diphenylpicrylhydrazyl, DPPH ($g = 2.0037$). ESI-MS mass spectra were obtained from the LC-TOF (KC-455) mass spectrometer of Waters.

2.3. Electrochemical measurements

Cyclic voltammetric experiments were performed using a CHI electrochemical analyzer (Model Nos. 600B or 1120A Series). The cell contained a glassy-carbon or a Pt working electrode, a Pt wire auxiliary electrode, and a saturated calomel electrode (SCE) reference electrode. A salt-bridge (containing supporting electrolyte, tetra *n*-butyl ammonium perchlorate (TBAP) dissolved in solvent of study) was used to connect the SCE with the electrochemistry solution [57]. For constant potential electrolysis experiments, a Pt-mesh was used as the working electrode. The solutions were ~1 mM in complex and ~0.1 M in supporting electrolyte TBAP. Under our experimental conditions, the $E_{1/2}$ value (in Volts) for the couple Fc^+/Fc was found to be 0.40 in MeCN versus SCE [58].

2.4. Crystallography

Single crystal X-ray diffraction intensities were collected for complexes **1** and **2** on a Bruker SMART APEX CCD diffractometer at 100(2) K using graphite-monochromated Mo Kα ($\lambda = 0.71073$ Å) radiation [59,60]. For complex **1**, a total of 25140 reflections were measured, of which 3354 were unique and 2457 were considered observed [$I > 2\sigma(I)$]. In case of complex **2**, a total of 40450 reflections were measured, of which 9529 were unique and 5686 were considered observed [$I > 2\sigma(I)$]. Intensity data were corrected for Lorentz and polarization effects but no absorption correction was applied [61]. The structures were solved by SIR-97 [62], expanded by Fourier-difference syntheses and refined with SHELXL-97 [63], incorporated in WINGX 1.64 crystallographic collective package [64]. Hydrogen atoms were placed in idealized positions and treated using riding model approximation with displacement parameters derived from those of the atoms to which they were bonded. All non-hydrogen atoms were refined with anisotropic thermal parameters by full-matrix least-squares procedures on F^2. The convergence was measured by the factors R and R_w, where $R = \sum(||F_o| - |F_c||)/\sum|F_o$ and $R_w = \{\sum[w(F_o^2 - F_c^2)^2]/\sum[w(F_o^2)^2]\}^{1/2}$. Details of the crystallographic data collection and structure solution parameters are summarized in Table 1.

2.5. Ligand syntheses

2.5.1. $H_2\mathbf{L}^H$

LiBr (0.66 g, 7.60 mmol), Na_2CO_3 (5.0 g, 38 mmol), and *N*,*N*′-bis(chloroacetyl)-*o*-phenylenediamine (1.01 g, 3.8 mmol) were taken in MeCN (150 mL) and the mixture was refluxed with stirring for 1 h. To this mixture was added *N*,*N*′-dimethyl propylenediamine (0.38 g, 3.8 mmol) dissolved in MeCN (50 mL). The resulting mixture was refluxed under stirring for an additional 48 h. The mixture was cooled, filtered and the solvent was removed under reduced pressure to afford a sticky solid. This product was further purified by the column chromatography using silica gel (100–200 mesh) with 5% MeOH–$CHCl_3$ ($R_f = 0.44$). A white product was obtained after the removal of solvent. Yield: 0.43 g (50%). An analytically pure product (in ~78% yield) can also be obtained by

Table 1
Crystallographic data collection and structural refinement parameters for [Ni($\mathbf{L}^H$)] (**1**) and [Ni($\mathbf{L}^{Cl}$)] (**2**).

Compounds	[Ni^{II}($\mathbf{L}^H$)] **1**	[Ni^{II}($\mathbf{L}^{Cl}$)] **2**
Empirical formula	$C_{15}H_{20}N_4O_2Ni$	$C_{15}H_{18}Cl_2N_4O_2Ni$
Formula mass	347.06	415.94
T (K)	100	100
Crystal system	monoclinic	monoclinic
Space group	$P2_1/c$	$P2_1/c$
Color, shape	yellow, prism	yellow, plate
a (Å)	9.608(5)	9.875(5)
b (Å)	15.584(5)	10.426(5)
c (Å)	10.479(5)	16.616(5)
α (°)	90.0(5)	90.0(5)
β (°)	103.882(5)	106.116(5)
γ (°)	90.0(5)	90.0(5)
V (Å^3)	1523.2 (12)	1643.5(12)
Z	4	4
$D_{calc.}$ (g cm^{-3})	1.513	1.681
Absorption coefficient (mm^{-1})	1.286	1.522
R[a]	0.0312	0.0427
R_w[b]	0.0737	0.1068
Goodness-of-fit (GOF) on F^2	1.025	0.995

[a] $R = \sum||F_o| - |F_c||/\sum|F_o|$.
[b] $R_w = \{[\sum(|F_o|^2|F_c|^2)^2]\}^{1/2}$.